Molecular Dynamics Simulations of Supported Phospholipid/Alkanethiol Bilayers on a Gold(111) Surface

Mounir Tarek,*# Kechuan Tu,* Michael L. Klein,* and Douglas J. Tobias§

*Laboratory for Research on the Structure of Matter, University of Pennsylvania, Philadelphia, Pennsylvania 19104-6202; #NIST Center for Neutron Research, Gaithersburg, Maryland 20899; and §Department of Chemistry, University of California, Irvine, California 92697-2025 USA

ABSTRACT Molecular dynamics simulations have been used to investigate the structure of hybrid bilayers (HB) formed by dipalmitoylphosphatidylcholine (DPPC) lipid monolayers adsorbed on a hydrophobic alkanethiol self-assembled monolayer (SAM). The HB system was studied at 20°C and 60°C, and the results were compared with recent neutron reflectivity measurements (Meuse, C. W., S. Krueger, C. F. Majkrzak, J. A. Dura, J. Fu, J. T. Connor, and A. L. Plant. 1998. *Biophys. J.* 74:1388) and previous simulations of hydrated multilamellar bilayers (MLB) of DPPC (Tu, K., D. J. Tobias, and M. L. Klein. 1995. *Biophys. J.* 69:2558; and 1996. 70:595). The overall structures of the HBs are in very good agreement with experiment. The structure of the SAM monolayer is hardly perturbed by the presence of the DPPC overlayer. The DPPC layer presents characteristics very similar to the MLB gel phase at low temperature and to the liquid crystal phase at high temperature. Subtle changes have been found for the lipid/water interface of the HBs compared to the MLBs. The average phosphatidylcholine headgroup orientation is less disordered, and this produces changes in the electric properties of the HB lipid/water interface. These changes are attributed to the fact that the aqueous environment of the lipids in these unilamellar films is different from that of MLB stacks. Finally, examination of the intramolecular and whole-molecule dynamics of the DPPC molecules in the fluid phase HB and MLB membranes revealed that the reorientations of the upper part of the acyl chains (near the acyl ester linkage) are slower, the single molecule protrusions are slightly damped, and the lateral rattling motions are significantly reduced in the HB compared with the MLB.

INTRODUCTION

Because of their potential use in a variety of applications such as biosensors, supported lipid membranes have been extensively studied (Tamm and McConnell, 1985; Tamm, 1988; Wright et al., 1988; Timbs and Thompson, 1990; Tien, 1990; Pisarchick and Thompson, 1990; Stelzle et al., 1993; Duschi et al., 1994). In the early investigations, model unilamellar phospholipid bilayers were supported on flat solid substrates, and were shown to be useful for probing the structure and dynamics of different inclusion compounds (Tamm and McConnell, 1985; Kalb et al., 1992; Duschi et al., 1994). In the last few years, new techniques have been developed to prepare supported bilayers by self-assembling lipid layers on the hydrophobic surface of Langmuir-Blodgett films (Florin and Gaub, 1993; Plant, 1993; Plant et al., 1994, 1995). Several methods have also been described to produce such hybrid bilayers (HB) using alkanethiol self-assembled monolayers (SAM) on gold surfaces. These supported HBs are very stable and are potentially very good candidates for membrane structure/function studies.

More recently, Meuse et al. (1998a) have used surface-enhanced Raman spectroscopy and reflection absorption infrared spectroscopy to study HBs composed of various alkanethiols ($C_6H_{13}SH$, $C_{10}H_{21}SH$, $C_{18}H_{37}SH$) and the lipids dipalmitoylphosphatidylcholine (DPPC) and dimyristoylphosphatidylcholine (DMPC). The phospholipids were shown to form well-ordered, noninterdigitated monolayers on top of the SAM. The overall structure of the HB was found to be consistent with previous investigations using other techniques (Plant, 1993; Plant et al., 1994). The SAM hydrophobicity apparently provides a driving force for the organization of the lipid overlayer, and the tail-to-tail attraction between the two layers stabilizes the overall structure, which has the lipid headgroups directed toward the air/water interface, away from the metal surface. The average conformation of the lipid monolayer alkane chains was shown to be very similar to that of a multilamellar lipid bilayer (MLB). Also, the structure of the SAM appeared to be only slightly altered by the presence of the phospholipid.

In a subsequent paper, Meuse et al. (1998b) used infrared spectroscopy and neutron reflectivity measurements to characterize the structure of the DPPC lipid overlayer in both dry and hydrated HBs. In the dry sample, the lipid forms a continuous monolayer that exhibits molecular order similar to that observed for MLBs. Furthermore, when hydrated, the HB retained its overall structure. Meuse et al. investigated the effect of temperature on the HB structure by analyzing neutron reflectivity measurements performed on different samples. Specifically, they studied the hydrated HB at 60°C (23° above the DPPC bilayer chain melting transition) and 20° (17° below). Measurements by Merkel et al. (1989) have shown that a supported bilayer based on DMPC exhibits a chain melting temperature that is ~4°C lower than for DMPC vesicles. Accordingly, we may assume that the HB systems at 60°C and 20°C correspond to liquid crystal-

Received for publication 29 January 1999 and in final form 13 May 1999.

Address reprint requests to Dr. Douglas J. Tobias, Department of Chemistry, University of California, Irvine, CA 92697-2025. Tel.: 949-824-4295; Fax: 949-824-8571; E-mail: dtobias@uci.edu.

0006-3495/99/08/964/09 $2.00

line and gel phases of DPPC, respectively. Meuse et al. showed that the HB is slightly thicker and more ordered at the lower temperature. The authors assumed in their analysis that the effect of temperature is to induce changes in the lipid monolayer structure. Moreover, it was not possible to accurately determine the water content near the lipid headgroup region. Overall, the best fit to the experimental data suggested that the lipid in the HB is much more hydrated than in the MLB. Moreover, in contrast to the situation for the MLB, there is only a minor change in hydration because of the temperature-induced gel → liquid crystal phase transition.

To gain additional insight into the properties of HB membrane mimetics at the molecular level, we have used molecular dynamics (MD) simulations. With this approach, it is possible using current generation atomistic force fields to provide an accurate description of MLBs and SAMs (Hautman et al., 1991). In the case of lipid bilayers, we have previously performed MD simulations on the DPPC liquid crystal L_α phase (Tu et al., 1995) and the gel phase (Tu et al., 1996). The fully hydrated MLBs were demonstrated to be stable and the structural properties of both phases compared favorably with the available experimental data. In this paper we report the results of applying similar MD protocols to simulate HBs composed of a DPPC monolayer adsorbed on an alkanethiol SAM in both liquid crystal and gel-like phases. We compare the present MD results with the available neutron data on "dry" and "hydrated" HBs in both phases, as well as to our previous DPPC bilayer simulations, and discuss the structural and dynamical properties of HBs in relation to those of pure MLBs.

MATERIALS AND METHODS

The initial SAM configuration was constructed from 64 octadecanethiol molecules at a surface area of 21.74 Å^2/chain following the procedure of Mar and Klein (1994). The SAM was equilibrated at 27°C during a 400-ps MD simulation at constant volume and temperature with two-dimensional periodic boundary conditions. The final structure was then used to generate the initial configuration of the HB systems. For the DPPC overlayers there is no direct experimental evidence as to whether or not the surface area/lipid molecule in HBs is different from that in MLBs. Therefore, as a first approximation we consider that they are similar. The initial configurations of the DPPC lipid monolayers were taken from well-equilibrated DPPC MLB simulations at 20°C (Tu et al., 1996) and 50°C (Tu et al., 1995). Although both of these systems contained 32 molecules/layer, they were characterized by different surface area/molecule. To set up the HB, periodic boundary conditions were used to generate SAMs with dimensions almost commensurate with the DPPC monolayers.

To adsorb the lipid layer on top of the SAM, the terminal methyl groups were gradually brought in contact. To study the effect of hydration on the structure of the HB bilayers, water molecules were included in the system. The initial water configurations were taken along with the corresponding DPPC monolayers from our previous bilayer simulations (Tu et al., 1995, 1996). For the simulation of the hydrated gel phase (20°C) an additional slab of water molecules was added so that both the gel and liquid crystal simulations contained 893 water molecules (28 water molecules/DPPC). The details of the resulting systems are summarized in Table 1.

At this point it is crucial to point out some of the shortcomings that result from this set-up. First, because we are considering a monolayer adsorbed on a solid surface, the area/molecule is fixed. This is not only affecting the structure of the SAM, which is known to slightly expand as the temperature rises (Fenter et al., 1993), but it also imposes a constraint that the surface area/lipid is fixed. Moreover, although we would prefer to have a SAM with dimensions commensurate with the lipid monolayer, considering that the system has to be of a relatively small size to be computationally tractable, this constraint was difficult to satisfy. For instance, the surface areas/lipid in the HB are 43.5 Å^2 and 61.2 Å^2 in our simulations at 20°C and 60°C, respectively, compared with the experimental values 47.2 Å^2/molecule (Tristram-Nagle et al., 1993) and 62 Å^2/molecule (Nagle et al., 1996). Although the high-temperature system is characterized by a lipid area/molecule very close to the experiment, the lipid surface area/molecule at low temperature is ~4% too low. Anticipating our results, we will see that this discrepancy is likely of minor significance to the lipid gel phase, because the tilt angle and the thickness of the lipid layer are similar to those in the MLB.

The MD calculations were carried out at constant temperature and volume. The temperature was controlled by the Nosé-Hoover chain method (Martyna et al., 1992), with separate thermostats on the SAM, the DPPC, and the water molecules. The extended system equations of motion were integrated with an iterative Verlet-like algorithm (Ciccotti and Ryckaert, 1986), using a time step of 1.0 fs, and the SHAKE algorithm (Ryckaert et al., 1977) was used to constrain the lengths of the bonds involving the hydrogen atoms. The fictitious masses of the thermostat variables were chosen according to the prescription given by Martyna et al. (1992) with time scales of 0.5 ps, and the Nosé-Hoover thermostat chain length was five.

The force field used for the DPPC molecules is the same as that used in our previous simulations of fully hydrated gel and liquid crystal L_α phase MLBs (Tu et al., 1995, 1996; Tobias et al., 1997a). The hydrocarbon portions of the SAM alkanethiol molecules were modeled using the potential of Tobias et al. (1997a), and the remainder of the alkanethiol force field was taken from Mar and Klein (1994), including the 12-3 adsorption potential and the surface corrugation potential to restrict the sulfur atoms to the threefold adsorption sites. The rigid three-site SPC/E potential (Berendsen et al., 1987) was used for water. All the parameters for the unspecified intermolecular interactions were obtained by using the Lorentz-Bertholot mixing rules.

Spherical truncation of the long-ranged electrostatic interactions is inappropriate for the highly polar system of interest here. In principle, a Ewald summation method suitable for a two-dimensional system with a finite extent in the third dimension (normal to the bilayer) could be used. However, to be computationally feasible, the extension of the system in the nonperiodic direction should be much less than in the periodic directions

TABLE 1 Details of the MD simulations

System	T (°C)	N_a	N_l	N_w	System size $X \times Y \times Z$ (Å)	Run length (ps)
SAM	20	64	—	—	40.1 × 34.7 × 200	400
Dry HBM	20	64	32	—	40.1 × 34.7 × 200	800
Hydrated HBM	20	64	32	893	40.1 × 34.7 × 200	500
Hydrated HBM	60	81	32	893	45.1 × 43.4 × 200	500

N_a, N_l, and N_w are, respectively, the number of alkanethiol, lipid, and water molecules in the system. The X and Y dimensions refer to a rectangular lattice.

(Hautman and Klein, 1992). Unfortunately, this criterion is not met by the system sizes used in the present study. We therefore used three-dimensional boundary conditions and took the length of the simulation cell in the direction normal to the bilayer to be large enough to ensure that the interactions between periodic replicas in this directions were insignificant (i.e., $Z = 200$ Å). The usual Ewald method (Allen and Tildesley, 1989) was used to calculate the electrostatic energies and forces. The minimum image convention was used to calculate the van der Waals interactions and the real space part of the Ewald sum with simple truncation at 10 Å.

RESULTS AND DISCUSSION

Instantaneous configurations from the simulations are displayed in Fig. 1 for three HBM systems, namely (*a*) dry, (*b*) hydrated gel-like phase, and (*c*) hydrated liquid-crystal-like phase. Fig. 1 shows that at 20°C there is very little change in the alkanethiol SAM structure on going from the dry to the hydrated state. However, when T is increased, the structure of the phospholipid changes significantly. As for the hydrated MLB, these changes are mainly characterized by a higher degree of disorder in the headgroup (P-N) dipole orientation and the melting of the hydrocarbon chains. With the increase in the area/molecule, the water molecules diffuse through the lipid interface leading to enhanced hydration of the phospholipid headgroup moieties, while the change in the hydrocarbon chain conformations results in a decrease in the overall layer thickness. In the following we will quantitatively characterize these changes. We will study the lipid structural properties in the HB as a function of the temperature, and compare them to the existing neu-

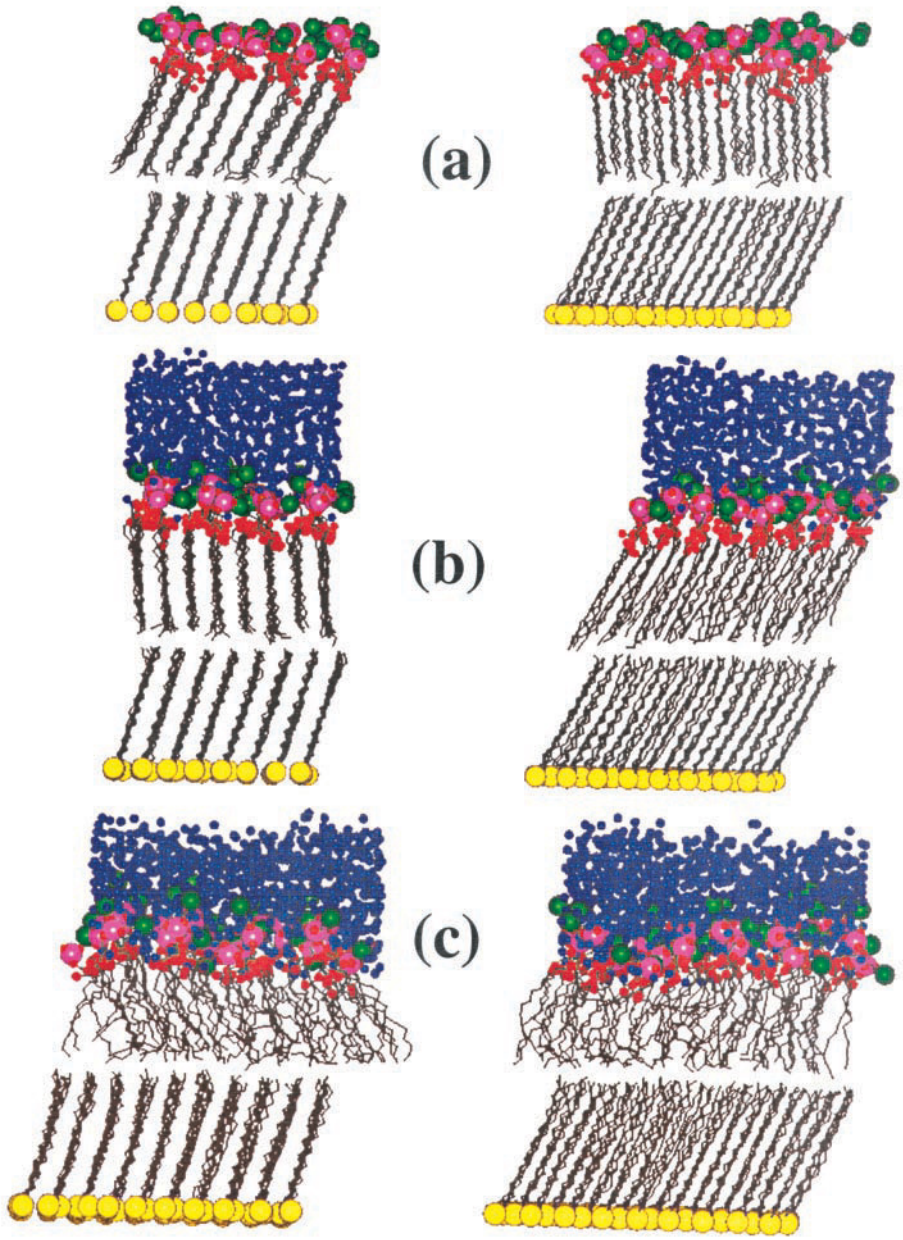

FIGURE 1 Orthogonal views of instantaneous configurations from the MD simulation left (*Z, X*) and right (*X, Y*). (*a*) Dry HBM; (*b*) hydrated HBM at 20°C; (*c*) hydrated HBM at 60°C. The sulfur atoms of the SAM (*yellow*) are represented by the van der Waals radius; the alkanethiol and the lipid hydrocarbon chains are represented by a ball-and-stick model. The P (*magenta*), N (*green*), carbonyl O (*red*), and water O (*blue*) atoms are represented by small spheres. All H atoms are omitted for clarity.

tron reflectivity measurements (Meuse et al., 1998b). Then, concentrating on the high-temperature liquid-crystalline phase, we will compare its structure to that of the hydrated MLB (Tu et al., 1995).

First, to monitor the changes in the SAM layer, we display in Fig. 2 the population of *gauche* conformations as a function of carbon number along the alkyl chain. This figure shows that at low temperature, the adsorption of the lipid layer onto the alkanethiol has little or no effect on the SAM hydrocarbon chain conformations. As for the pure SAM monolayer, the middle of the chain is almost defect-free, and there are few *gauche* conformations around the terminal methyl group. Except for the terminal methyl group, which shows more disorder, there appears to be no measurable difference between the pure SAM and the alkanethiol monolayer in the HB. For the high-temperature phase, the changes in the number of *gauche* along the alkanethiol hydrocarbon chains is similar to that observed for the pure SAM (Mar and Klein, 1994). The measurable increase through the chain of the *gauche* population indicates an overall disorder of the alkanethiol chain conformation.

We have also studied the mean tilt of the SAM hydrocarbon chains. The tilt was calculated as the angle between the C3-C15 carbon segment and the normal to the gold surface. Fig. 3 displays the tilt angle distribution, which shows again that the structure of the SAM is not altered by the presence of the lipid overlayer at room temperature in either the dry or the hydrated samples. The mean tilt estimated from the simulations at 20°C are 31.0 ± 5.0°, 30.5 ± 5.0°, and 31.5 ± 5.0° for the pure SAM, the dry HB, and the hydrated HB systems, respectively. At higher temperature, i.e., 60°C, in agreement with previous results (Mar and Klein, 1994), the tilt angle decreases slightly for the pure alkanethiol SAM to 28.5 ± 5.0°. However, in the presence of the lipid overlayer the distribution shifts to slightly lower angles (27.5 ± 8.0°) and also broadens, reflecting a higher disorder of the chains.

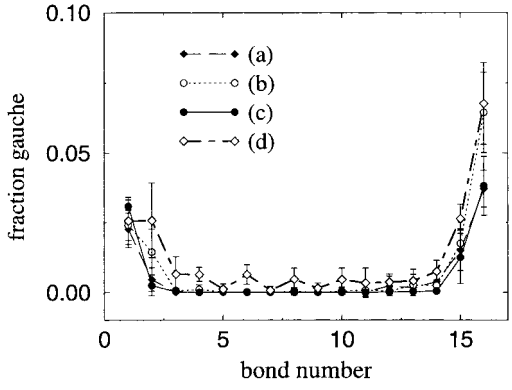

FIGURE 2 Fraction *gauche* conformations versus bond number in the alkanethiol SAM. (*a*) Pure SAM; (*b*) dry HBM; (*c*) hydrated HBM at 20°C; (*d*) hydrated HBM at 60°C. The error bars are represented by $\pm\sigma$, where σ is the standard deviation computed over blocks of 50 ps.

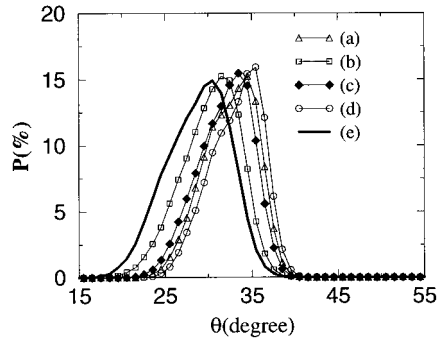

FIGURE 3 Alkanethiol tilt angle probability distribution. (*a*) Pure SAM at 20°C; (*b*) pure SAM at 60°C; (*c*) dry HBM at 20°C; (*d*) hydrated HBM at 20°C; (*e*) hydrated HBM at 60°C.

By monitoring the surface-enhanced Raman spectra of the SAM at room temperature, Meuse et al. (1998a) were able to demonstrate that the lipid overlayer induces ordering for short alkanethiol chains (hexanethiol), while no noticeable change was detected for the longer octadecanethiol. From reflectance absorption IR spectra, in agreement with Snyder et al. (1986), these authors conclude that the ordering of the chains is mainly due to changes in the low-frequency torsional modes and not to conformational changes (*gauche* defects) along the alkanethiol chain. A thorough analysis of the changes induced in torsional modes is beyond the scope of this study, because the force field used is well-known to give only an approximate description of these modes. However, the present MD study confirms the lack of conformational changes in the SAM, which is in agreement with the spectroscopic data.

To compare the present simulation results to the neutron reflectivity measurement of Meuse et al. (1998b), we calculated the number density profiles of the HB components for the hydrated samples at low and high temperature. Fig. 4 displays the individual densities of the sulfur atom, the SAM, and phospholipid hydrocarbon chains (C and H atoms), the carbonyl, phosphate, and choline groups of the lipid headgroup, and the water. These densities are rescaled for clarity. As previously discussed for the SAM hydrocarbon chain, increasing the temperature induces conformational disorder along the chain and therefore leads to a smoothing of the density profiles. The density profile of the phospholipid alkyl chains shows that at both temperatures the lipid is noninterdigitating with the SAM. As for the MLB, in the higher temperature liquid-crystalline HB phase, the phospholipid density components are more smeared out, and the thickness of the phospholipid layer is diminished relative to the lower-temperature gel-like phase.

A more quantitative comparison of the DPPC density values is not possible because they were not extracted from the neutron reflectivity data of Meuse et al. (1998b). Furthermore, in the case of the gel phase, the experimental system is expected to have an appreciable density of defects (Merkel et al., 1989), while the simulated system is defect-free. The defects may arise because of the chain tilting

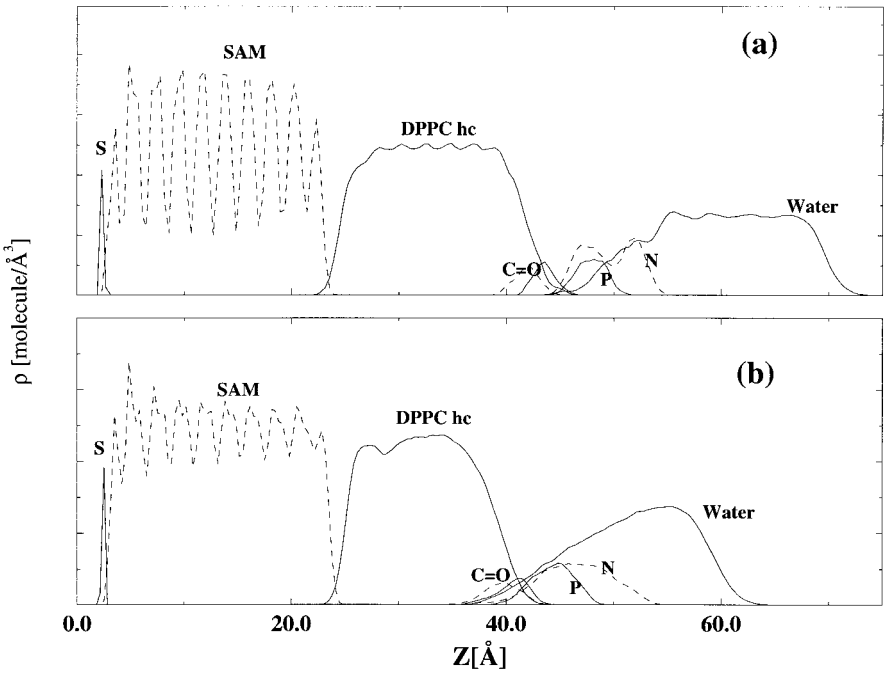

FIGURE 4 Number density profiles along the HBM normal z, averaged over the simulations. (*a*) Hydrated HBM at 20°C; (*b*) hydrated HBM at 60°C. Separate contributions from the SAM alkanethiol, the DPPC hydrocarbon (hc) chain, chemical moieties in the DPPC acyl ester regions (C═O) and the headgroup (P, N), and the water layer are displayed.

and/or because of the incommensurability of the SAM and DPPC hydrocarbon chain lattices.

The most significant change in the HB number densities is that the profile for the choline group evolves from a bimodal distribution at 20°C to a broad unimodal distribution at 60°C. To compare the characteristics of the HB individual distributions to the models used by Meuse et al. (1998b) in fitting the reflectivity data, we estimated the thickness of the SAM, the lipid hydrocarbon chain, and the lipid headgroup from the number density profiles. Here, the thickness has been defined as the region where the number density is higher than 50% of the maximum density. The estimates from the density plots, reported in Table 2, compare very well with fits to the neutron data. We note that although the tilt angle of the alkanethiol chains has increased by ~6°, the thickness of the layer did not change by >1 Å. This small value is within the error bar of the experimental data and agrees with the assumptions of Meuse et al. (1998b). The structure of the lipid layer is also in very good agreement with the neutron reflectivity measurements. Trends similar to the MLB structure are found, namely an increase of the headgroup thickness as the temperature increases. Hence, despite the constraints on the surface area/molecule imposed in the MD calculations, the analysis shows that the simulation reproduces the characteristics of the HB that emerge from the recent neutron measurements rather well. Taken together, the results validate the assumptions used in the experimental data reduction and the potential parameters used in the calculations.

In the following we will develop a molecular picture of the lipid layer to probe structural differences with the pure MLBs. First, we study the alkyl chains. The hydrocarbon chain structure is often described in terms of S_{CD}, the deuterium order parameters. $S_{CD} = \frac{1}{2}\langle 3\cos^2\theta - 1\rangle$, where θ is the angle between the C-D bond in the methylene group and the bilayer normal, is proportional to the quadrupolar splitting in deuterium NMR experiments (Seelig and Seelig, 1974). In a previous publication we underlined the fact that although the MD calculation gives correct bilayer dimensions and density, it is difficult to quantitatively reproduce the order parameters along the lipid chains. For instance, in the MLB L_α lipid phase (Tu et al., 1995), our previous calculations predicted too much order at both ends of the chains. In Fig. 5 we report the values of S_{CD} as a function of carbon number averaged over the lipid *Sn*1 and *Sn*2 chains and compare the results to the previous L_α MLB phase simulation. The estimated standard deviations of ~±0.02 are omitted for clarity. Fig. 5 shows that the HB

TABLE 2 Estimated thickness (Å) of the headgroup (HG) and the hydrocarbon chain (C) regions of the hybrid bilayer

System	Reference	DPPC (HG)	DPPC (C)	SAM (C)
Hydrated HB (20°C)	This work	12.0 ± 0.5	17.0 ± 0.5	20.0 ± 0.5
	Meuse et al. (1998b)	13.0 ± 1.0	15.7 ± 0.5	19.8* ± 1.0
Hydrated HB (60°C)	This work	10.0 ± 0.5	14.0 ± 0.5	19.0 ± 0.5
	Meuse et al. (1998b)	10.0 ± 1.0	13.2 ± 0.5	19.9* ± 1.0

*Value deduced from the overall thickness of the HB film and the thickness of the lipid hydrocarbon chain region.

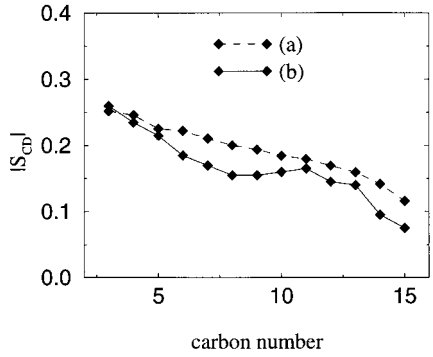

FIGURE 5 Comparison of simulation results of the lipid hydrocarbon chain deuterium parameters. (*a*) MLB at 50°C (Tu et al., 1995) and (*b*) HBM at 60°C (this work). The standard deviations ($\simeq \pm 0.02$) are not represented for clarity.

lipid is characterized by more disorder toward the end of the chains. As the temperature of the present system is 10°C higher than the MLB simulation, it is likely that the greater chain conformational disorder is mainly temperature-induced.

To investigate the structure of the lipid-water interface, in Fig. 6 we compare the electron density profiles for the DPPC and water layers in the HB (60°C) and the MLB (50°C) systems (Tu et al., 1995). Fig. 6 clearly shows large differences between the two systems at the molecular level. These differences are mainly related to the orientation of the lipid headgroups and the extent of water penetration into the polar region. For further analysis we calculated the headgroup orientation with respect to the normal $\vec{n}$ to the lipid layer. Displayed in Fig. 7 are the probability distribution of the θ angle between the P-N vector and $\vec{n}$. As previously discussed by Tu et al. (1995), the main difference between the gel and the liquid crystal phases for the lipid MLBs is the presence in the gel phase of a double peak orientational distribution. This bimodal distribution also appears in the choline group electron (number) density profile. For the high-temperature phase (lower surface density), the lipid headgroup orientation is more uniform, and a large fraction of the molecules point their dipole toward the interior of layer ($\theta > 90°$). For the HB system, the bimodal distribution of the choline group density profile is maintained in the gel phase; however, the difference in the PN orientation distribution between 20°C and 60°C is less remarkable. In both cases only a minor fraction of the molecules orient their dipole toward the hydrocarbon core.

Reorientational motions of phospholipid headgroups occur on a time scale of ~1 ns (Tobias et al., 1997b). One might argue, therefore, that the PN angular distributions calculated here are not converged well enough. However, it should be recalled that we started from lipid configurations taken from our previous equilibrated DPPC MLB simulations (Tu et al., 1995, 1996). Thus, for both systems (20°C and 60°C) the length of the present simulation was likely long enough to allow for any desired reorientation of the lipid headgroups. Given that the present simulation of the liquid-crystal-like HB was performed at a higher temperature compared with Tu et al. (1995), one might expect that the PN dipole would be even more randomly distributed, but this is clearly not the case. The observed changes are probably the result of the absence of headgroup-headgroup interactions and packing across the water slab that are present in the stacked arrangement of the MLB simulation. Indeed, in the HB systems considered here, the lipid head-

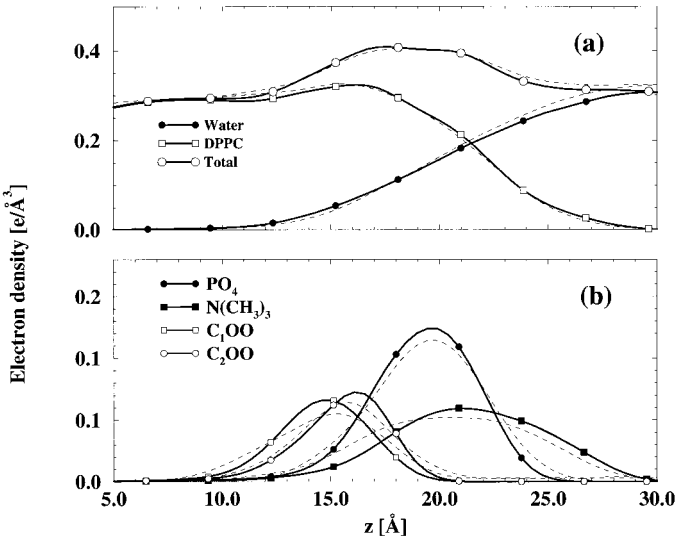

FIGURE 6 Electron density profiles along the bilayer normal *z* averaged over the simulations. (*a*) Total electron density for the water, the DPPC, and their sum; (*b*) separate contributions from the headgroup and acyl ester regions of the DPPC molecules. The broken lines represent the results from the MLB simulation at 50°C (Tu et al., 1995), and the solid line the HBM system at 60°C (present work). For the purpose of comparison, the MLB profiles have been collectively shifted along *z*.

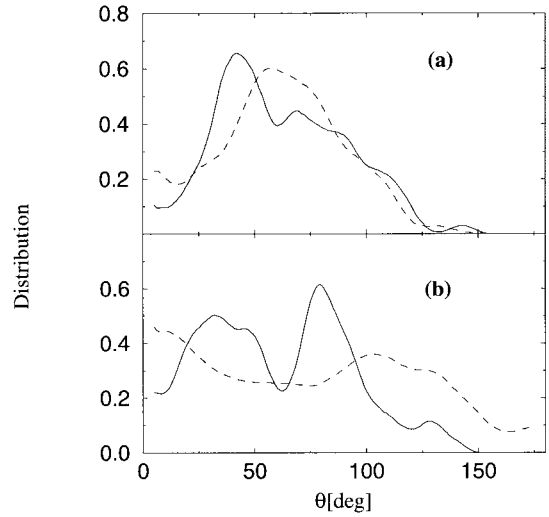

FIGURE 7 DPPC PN dipole orientational distribution with respect to the normal to the bilayer. The broken and solid lines are, respectively, T = 60°C and 20°C for the HBM system (*a*), and T = 50°C and 20°C for the MLB system (*b*) (Tu et al., 1995, 1996).

groups are in an environment more like that in a single-walled vesicle.

The lipid "hydration" may be defined in several ways, depending on the level of description. In neutron and x-ray experiments the lipid hydration (defined as the number of water molecules associated with the phosphatidylcholine headgroup) is calculated from the thickness and an estimate of the specific volume of the lipid headgroup. Meuse et al. (1998b) have estimated that these numbers are higher for the HB compared with the MLBs (Nagle et al., 1996; Sun et al., 1994). Furthermore, the authors found no major difference in the degree of lipid hydration between the high- and low-temperature HB phases ($\simeq$11 water/lipid). A direct calculation from the MD simulation can be achieved by cumulative integration of the water number density profiles (Fig. 4) i.e., counting the number of water molecules located in the headgroup region. Considering that the headgroup region expands in the Z direction ($\vec{n}$) up to the limit where the number density of the nitrogen atom falls to half its maximum value, the hydration numbers are, respectively, 10.5 ± 0.5 and 5.0 ± 0.5 water/lipid molecules for the high- and low-temperature HBs. These numbers are somewhat arbitrary because they depend on the definition of the headgroup region. However, because we compare the two systems similarly, the estimated numbers indicate that the HB lipid layer is much less "hydrated" in the low-temperature gel-like phase than at the high-temperature liquid-crystalline-like phase. Using the same criterion, we calculated the hydration of the lipid headgroup for the L_α MLB phase (Tu et al., 1995). The value found (12.5 ± 0.5 water/lipid) suggests that, in contradiction with Meuse et al. (1998b), the lipid headgroups in the HB are, for comparable temperatures, in a state of hydration similar to that of pure lipid multilayers, albeit with slightly lower hydration.

Another property that we may address using the simulation is the electric potential difference V across the lipid/water interface. In fact, there is an appreciable potential difference across lipid/water interfaces, typically a few hundred millivolts, negative on the water side relative to hydrocarbon. Reports of experimentally measured values of this "dipole potential" range from -200 mV to -500 mV, depending on the system and type of measurements (Gawrisch et al., 1992; Flewelling and Hubbell, 1986). It is possible to estimate these potentials from MD simulations, given some crude assumptions. Usually, V is calculated as a double integral of molecular charge density distributions, neglecting the explicit electronic polarization. Tobias et al. (1997a) have estimated the values of the total potential across the lipid/water interface for DPPC in the L_α MLB phase. According to their calculation, the total potential arises primarily due to an excess of water molecules oriented with their dipole pointing toward the membrane surface, while the contribution from the DPPC headgroup cancels through the interface. The overall potential amounts to ~ -500 mV. We have calculated the dipole potential across the lipid/water interface for the liquid crystal phase HB system in a similar way. Averaged over the simulation, we find first that there is a net contribution from the lipid of $\simeq -100$ mV because of the particular orientational distribution of the PN dipole. Second, the contribution from water amounts only to $\simeq -220$ mV, leading to a total of $\simeq -320$ mV. As previously noted (Tu et al., 1998), these results underline the connection between subtle structural changes and nontrivial modifications of the electric properties of the bilayers. Regardless of the accuracy of the estimates and the assumptions made, the present results suggest that the electric properties of the lipid/water interface under consideration are different from those of lipid MLB systems.

On time scales ranging from one to several hundred picoseconds, lipid molecules in bilayers exhibit a variety of whole-molecule and internal motions with amplitudes of a few angstroms (König and Sackmann, 1996), including single molecule protrusions and lateral "rattling in a cage" dynamics, and complicated rearrangements of the acyl chains. The protrusions may play a role in determining the repulsive "hydration" force of a membrane surface (Lipowski and Grotehans, 1993), and the rattling-and-chain conformational dynamics contribute to the microscopic viscosity (Venable et al., 1993); hence, the transport properties of the membrane interior. In light of the potential uses of HB membranes in biophysical and materials applications, it is of interest to characterize the dynamics of the lipids in these films, and compare them with the situation in pure lipid MLBs.

The internal dynamics of the hydrocarbon chains, or "fluidity" of the bilayer interior, is conveniently discussed in terms of the correlation functions $C(t) = \frac{1}{2}\langle 3[\mu(t) \cdot \mu(0)]^2 - 1\rangle$, where μ is a unit vector along the methylene C-H bond. These correlation functions describing the reorientational relaxation of the acyl chains generally consist of a fast ($\simeq$100 ps) and slow ($>$1 ns) component. In Fig. 8 *A* we display $C(t)$ for the DPPC molecules in the HB and the MLB phases at 50°C and 60°C, respectively. This figure indicates that the reorientation is slightly slowed for the HBM near the top of the chain (carbon C2) but not affected elsewhere. This result suggests that the microscopic "fluidity" of the lipid layer is preserved. The correlation functions represent a superposition of several chain motions occurring at the 100-ps time scale. These include kink formation, disappearance, and diffusion, as well as simpler motions such as *trans-gauche* isomerization. Fig. 8 *B* shows the rates of *trans-gauche* isomerization, suggesting that these small-amplitude motions are also similar in the two systems.

The internal dynamics of the hydrocarbon chains, or "fluidity" of the bilayer interior, is conveniently discussed in terms of the time correlation functions, $C(t) = \frac{1}{2}\langle 3[\mu(t) \cdot \mu(0)]^2 - 1\rangle$, where μ is a unit vector along a methylene C-H bond. The results plotted in Fig. 8 *B* show that the reorientational motion as reflected by the decay of $C(t)$ is significantly slower in the HB compared with the MLB for the upper part of the chain near the acyl ester linkage (e.g., C2), slightly slower in the middle of the chain (e.g., C8), and unchanged at the end of the chain (e.g., C15). The $C(t)$ in Fig. 8 *A* represent a superposition of all of the chain motions

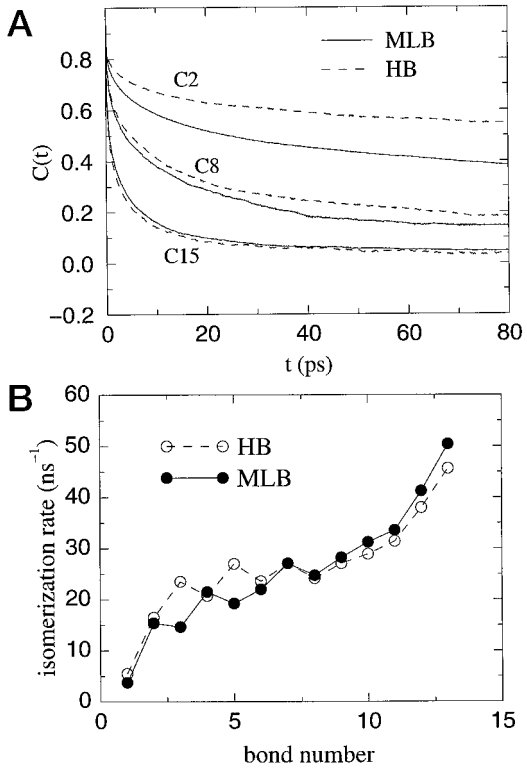

FIGURE 8 (*A*) Orientational time correlation functions $C(t) = \langle P_2[\mu(0) \cdot \mu(t)]\rangle$ for selected C-H vectors, μ, in the DPPC acyl chains computed from simulations of a pure DPPC MLB at 50°C (*solid lines*) and a DPPC/alkanethiol HB at 60°C (*dashed lines*). (*B*) Rates of *trans-gauche* transitions as functions of the bond number in the DPPC acyl chain in the MLB (*filled circles, solid lines*) and HB (*open circles, dashed lines*).

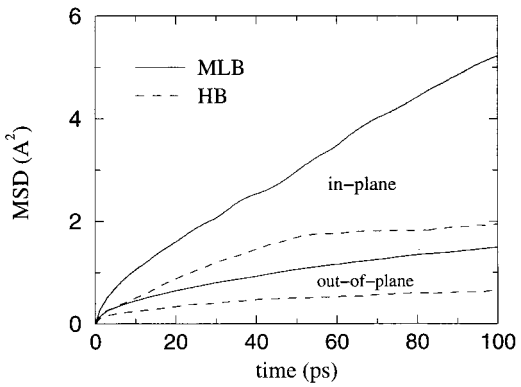

FIGURE 9 Center-of-mass mean-squared displacements of DPPC molecules in the plane of the bilayer (*top two curves*) and perpendicular to the plane (*bottom two curves*) from simulations of a pure DPPC MLB 50°C (*solid lines*) and a DPPC/alkanethiol HB at 60°C (*dashed lines*).

occurring on the 100-ps time scale, including simple *trans-gauche* isomerizations as well as more complicated rearrangements such as kink formation, disappearance, and diffusion. To isolate the simple isomerizations, we have calculated the rates of *trans-gauche* transitions as described by Venable et al. (1993). The results plotted in Fig. 8 *B* show that there is little difference in the isomerization rates between the MLB and HB membranes.

The whole-molecule rattling and protrusion of the DPPC molecules can be qualitatively discussed in terms of the DPPC center-of-mass mean-squared displacements (MSD) in and out of the plane of the bilayer, respectively. The results in Fig. 9 predict that the protrusions are slightly quenched in the HB compared with the MLB, as expected for a DPPC monolayer adsorbed on the flat SAM surface. In addition, the simulations also predict, somewhat surprisingly, that the in-plane motion is markedly reduced in the HB relative to the MLB.

CONCLUSION

We have performed a series of MD simulations on both dry and hydrated alkanethiol/DPPC HBMs. In the latter case we studied the low- (20°C) and high- (60°C) temperature "phases" of the lipid overlayer and made extensive comparison with the results of experiments and previous simulations of gel and liquid crystal phases of DPPC MLBs (Tu et al., 1995, 1996). In agreement with spectroscopic results (Meuse et al., 1998a) we found that the alkanethiol SAM structure is essentially unperturbed by the presence of the lipid overlayer.

The lipid of the HB exhibits overall structures very similar to those of the pure MLB assemblies. Specifically, the order and packing characteristics of a gel phase at the lowest temperature and the liquid crystal L_α phase at higher temperature. The thickness of the SAM, the lipid hydrocarbon chain, and the phosphatidylcholine headgroup regions were in very good agreement with the values extracted from neutron reflectivity measurements (Meuse et al., 1998b) both at 20°C and 60°C.

Comparing the structures of the HB and MLB systems, the study revealed subtle changes, mainly in the headgroup orientational distribution. For instance, in the high-temperature phase the distribution of the PN dipole is much narrower than found in the MLB. This more ordered headgroup packing gives rise to a modification of the lipid/water interfacial structure, clearly changing the electrostatic potential across the interface. However, this change seems to only slightly affect the "hydration" characteristics of the phosphatidylcholine headgroup, in contrast to what has been postulated in the literature (Meuse et al., 1998b). The changes in the water/lipid HB interface may be explained by the fact that it is characterized by an aqueous environment similar to that of a single isolated membrane, such as found in unilamellar vesicles, while in multilamellar stacks, headgroup-headgroup interactions across the water slab appear to alter the properties of the interface.

Finally, our simulations revealed some differences in the intramolecular and whole-molecule dynamics of the DPPC molecules in the fluid phase HB and MLB membranes. In particular, the reorientations of the upper part of the acyl chains (near the acyl ester linkage) are slower, the single molecule protrusions are slightly damped, and the lateral

rattling motions are significantly reduced in the HB compared with the MLB.

We thank Anne Plant, Susan Krueger, and Curtis Meuse for many helpful discussions. K.T. benefited from a National Science Foundation summer internship at the National Institute for Standards and Technology.

This research was supported by a cooperative research agreement between the National Institute for Standards and Technology and the LRSM, and in part by the University of Pennsylvania MRSEC under National Science Foundation Grant DMR 96-32598. D.J.T. was supported in part by start-up funds provided by the University of California, Irvine.

REFERENCES

Allen, M. P., and D. J. Tildesley. 1989. Computer Simulation of Liquids. Oxford University Press, New York.

Berendsen, H. J. C., J. R. Grigera, and T. P. Straatsma. 1987. The missing term in effective pair potentials. *J. Phys. Chem.* 91:6269–6271.

Ciccotti, G., and J.-P. Ryckaert. 1986. Molecular dynamics simulation of rigid molecules. *Comp. Phys. Rep.* 4:345–392.

Duschi, C., M. Liley, G. Corradin, and H. Vogel. 1994. Biologically addressable monolayer structures formed by templates of sulfur-bearing molecules. *Biophys. J.* 67:1229–1237.

Fenter, P., P. Eisenberger, and K. S. Liang. 1993. Chain-length dependence of the structures and phases of $CH_3(CH_2)_{n-1}SH$ self-assembled on Au(111). *Phys. Rev. Lett.* 70:2447–2450.

Flewelling, R. F., and W. L. Hubbell. 1986. The membrane dipole potential in a total membrane potential model. *Biophys. J.* 49:541–552.

Florin, E.-L., and H. E. Gaub. 1993. Painted supported lipid membranes. *Biophys. J.* 64:375–383.

Gawrisch, K. D., D. Ruston, J. Zimmerberg, V. A. Parsegian, R. P. Rand, and N. Fuller. 1992. Membrane dipole potential, hydration forces, and the ordering of water at membrane surface. *Biophys. J.* 61:1213–1223.

Hautman, J., J. P. Bareman, W. Mar, and M. L. Klein. 1991. Molecular dynamics investigations of self-assembled monolayers. *J. Chem. Soc. Faraday Trans.* 87:2031–2037.

Hautman, J., and M. L. Klein. 1992. A Ewald summation method for planar surfaces and interfaces. *Mol. Phys.* 75:379–395.

Kalb, E., S. Frey, and L. K. Tamm. 1992. Formation of supported planar bilayers by fusion of vesicles to supported phospholipid monolayers. *Biochim. Biophys. Acta.* 1103:307–316.

König, S. and E. Sackmann. 1996. Molecular and collective dynamics of lipid bilayers. *Curr. Opin. Colloid Interface Sci.* 1:78–82.

Lipowski, R., and S. Grotehans. 1993. Hydration versus protrusion forces between lipid bilayers. *Europhys. Lett.* 23:599–604.

Mar, W., and M. L. Klein. 1994. Molecular dynamics study of the self-assembled monolayer composed of $S(CH_2)_{14}CH_3$ molecules using an all-atoms model. *Langmuir*. 10:188–196.

Martyna, G. J., M. L. Klein, and E. Tuckerman. 1992. Nosé-Hoover chains: the canonical ensemble via continuous dynamics. *J. Chem. Phys.* 97: 2635–2643.

Merkel, R., E. Sackmann, and E. Evans. 1989. Molecular friction and epitactic coupling between monolayers in supported bilayers. *J. Phys. (France)*. 50:1535–1555.

Meuse, C. W., G. Niaura, M. L. Lewis, and A. L. Plant. 1998a. Assessing the molecular structure of alkanethiol monolayers in hybrid bilayer membranes with vibrational spectroscopies. *Langmuir.* 14:1604–1611.

Meuse, C. W., S. Krueger, C. F. Majkrzak, J. A. Dura, J. Fu, J. T. Connor, and A. L. Plant. 1998b. Hybrid bilayer membranes in air and water: infrared spectroscopy and neutron reflectivity studies. *Biophys. J.* 74: 1388–1398.

Nagle, J. F., R. T. Zhang, S. Tristram-Nagle, W. J. Sun, H. Petrache, and R. M. Suter. 1996. X-ray structure determination of fully hydrated Lα phase dipalmitoylphosphatidylcholine bilayers. *Biophys. J.* 70: 1419–1431.

Pisarchick, M. L., and N. L. Thompson. 1990. Binding of a monoclonal antibody and its FAB fragment to supported phospholipid monolayers measured by total internal reflection fluorescence microscopy. *Biophys. J.* 58:1235–1249.

Plant, A. L. 1993. Self-assembled phospholipid/alkanethiol biomimetic bilayers on gold. *Langmuir*. 9:2764–2767.

Plant, A. L., M. Brighamburke, E. C. Petrella, and D. J. Oshannessey. 1995. Phospholipid alkanethiol bilayers for cell-surface receptors studies by surface plasmon resonance. *Anal. Biochem.* 226:342–348.

Plant, A. L., M. Gueguetchkeri, and W. Yap. 1994. Supported phospholipid/alkanethiol biomimetic membranes: insulating properties. *Biophys. J.* 67:1126–1133.

Ryckaert, J. P., G. Ciccotti, and H. J. C. Berendsen. 1977. Numerical integration of the Cartesian equations of motion of a system with constraints: molecular dynamics of n-alkanes. *J. Comp. Phys.* 23: 327–341.

Seelig, A., and V. Seelig. 1974. Dynamic structure of fatty acyl chains in a phospholipid bilayer measured by DMR. *Biochemistry*. 13: 4839–4845.

Snyder, R. G., M. Maroncelli, H. L. Strauss, and V. M. Hallmark. 1986. Temperature and phase behavior of infrared intensities: the poly(methylene) chain. *J. Phys. Chem.* 90:5623–5630.

Stelzle, M., G. Weissmuller, and E. Sackmann. 1993. On the application of supported bilayers as receptive layers for biosensors with electrical detection. *J. Phys. Chem.* 97:2974–2981.

Sun, W.-J., R. M. Suter, M. A. Knewtson, C. R. Worthington, S. Tristram-Nagle, R. Zhang, and J. F. Nagle. 1994. Order and disorder in fully hydrated unoriented bilayers of gel phase dipalmitoylphosphatidylcholine. *Phys. Rev. E.* 49:4665–4676.

Tamm, L. K. 1988. Antibody binding to lipid model membranes. The large ligand effect. *Biochemistry*. 27:7453–7458.

Tamm, L. K., and H. M. McConnell. 1985. Supported phospholipid bilayers. *Biophys. J.* 47:105–113.

Tien, H. T. 1990. Self-assembled lipid bilayers for biosensors and molecular electronic devices. *Adv. Mater.* 2:316–318.

Timbs, M. M., and N. L. Thompson. 1990. Slow rotational motions of antibodies on supported phospholipid monolayers measured by polarization-sensitive fluorescence photobleaching recovery. *Biophys. J.* 58: 413–428.

Tobias, D. J., K. Tu, and M. L. Klein. 1997a. Assessment of all-atom potentials for modeling membranes: molecular dynamics simulations of solid and liquid alkanes and crystals of phospholipid fragments. *J. Chim. Phys. Phys.-Chim. Biol.* 94 1482–1502.

Tobias, D. J., K. Tu, and M. L. Klein. 1997b. Atomic-scale molecular dynamics simulations of lipid membranes. *Curr. Opin. Colloid Interface Sci.* 2:15–26.

Tristram-Nagle, S., R. Zhang, R. M. Suter, C. R. Worthington, W.-J. Sun, and J. F. Nagle, 1993. Measurement of chain tilt angle in fully hydrated bilayers of gel phase lecithins. *Biophys. J.* 64:1097–1109.

Tu, K., M. L. Klein, and D. J. Tobias. 1998. Constant-pressure molecular dynamics investigation of cholesterol effects in a DPPC bilayer. *Biophys. J.* 75:2147–2156.

Tu, K., D. J. Tobias, and M. L. Klein. 1995. Constant pressure and temperature molecular dynamics simulation of a fully hydrated liquid crystal phase dipalmitoylphosphatidylcholine bilayer. *Biophys. J.* 69: 2558–2562.

Tu, K., D. J. Tobias, and M. L. Klein. 1996. Molecular dynamics investigation of the structure of a fully hydrated gel phase dipalmitoylphosphatidylcholine bilayer. *Biophys. J.* 70:595–608.

Venable, R. M., Y. Zhang, B. J. Hardy, and R. W. Pastor. 1993. Molecular dynamics simulations of a lipid bilayer and of hexadecane: an investigation of membrane fluidity. *Science*. 262:223–226.

Wright, L. L., A. G. Palmer, and N. L. Thompson. 1988. Inhomogeneous translational diffusion of monoclonal antibodies on phospholipid Langmuir-Blodgett films. *Biophys. J.* 54:463–470.